

Sensitivity Analysis in Mathematical Models of the Hypothalamus-Pituitary-Thyroid Axis

CLARA HORVATH, ANDREAS KÖRNER
Institute of Analysis and Scientific Computing
TU Wien
Wiedner Hauptstraße 8
Vienna, AUSTRIA

Abstract: Mathematical models are promising and important for advancing the current medical practice in the field of endocrinology. To assess the reliability of the range of mathematical models describing the hypothalamus-pituitary-thyroid axis and to establish their applicability in clinical decision support, we conducted a local and global sensitivity analysis of the model. Thyroid regulation in euthyroid and diseased individuals may be quantified and dynamic behavior predicted through mathematical models, thereby revolutionizing the current clinical practice. We investigated the influence of model parameters of a selected mathematical model utilizing ordinary differential equations describing the HPT-axis. Motivated by a graphical depiction of the varying influence of the model parameters, feasible methods such as a local sensitivity analysis are conducted. Furthermore, to account for the influence of parameters on the output variance of the considered model, the theory of Sobol' indices is utilized. Although the system of differential equations describing the hormone concentrations of thyroid-simulating hormones and unbound Thyroxine has similar equation structures, the results of the sensitivity analyses varied according to the equation.

Key-Words: Mathematical Modeling, Hypothalamus-Pituitary-Thyroid Axis, Local Sensitivity Analysis, Global Sensitivity Analysis, Ordinary Differential Equations

Received: May 25, 2024. Revised: June 29, 2024. Accepted: September 12, 2024. Published: October 8, 2024.

1 Introduction

Thyroid diseases affect an estimated 200 million people globally, with an additional 60% of those affected believed to be undiagnosed, making this an increasingly important area of research [1], [2]. A promising approach to gain insight into the functional interactions of the thyroid gland lies within the field of mathematical modeling. Throughout the years of research varying mathematical modeling approaches were utilized to describe aspects of the endocrine system such as the functionality of the thyroid gland.

In general, the feedback loop of hormonal signals starts in the hypothalamus, continues to the pituitary gland and terminates in a specific target gland. In the case of the thyroid gland, models consisting of systems of differential equations were established to describe this process. A prominent model was introduced by DiStefano et al. [3], which describes the course of thyroid hormone concentrations over time using a large system of differential equations. Additionally, a sub-model was incorporated to explore the effects of oral medication in the case of hypothyroidism, a condition in which the thyroid gland does not produce enough thyroid hormones. Berberich et al. [4] investigated how their model accounts for the influence of the circadian rhythm on the functionality of the thyroid gland. Furthermore, the interaction between various organs, such as liver and heart are also included to better understand

hormone homeostasis. Making [4] a rare exception, a sensitivity analysis was conducted as well. A very recent contribution includes Pompa et al. [5] with their work on compartment models. The functionality of the thyroid gland is described by including concentrations of thyrotropin-releasing hormone and thyroglobulin with additionally considering the effect of iodine in the modeling process. Also utilizing differential equations, Leow [6] proposed an exponential connection between hormones of the pituitary and thyroid gland. Utilizing approaches from control theory, Sharma et al. [7] introduce an approach to introduce an automated dosage recommendation of levothyroxine for patients suffering from Hashimoto's Thyroiditis.

However, thorough analysis of the mathematical properties of these models, although crucial for their clinical reliability, is missing. To better understand the underlying properties of the considered mathematical models, we conducted a sensitivity analysis of a model introduced in [8]. Based on this analysis, the reliability of a model and its usability in clinical decision support can be established. To offer a comprehensive treatment of the topic, the biological mechanisms underlying the endocrine system and the theoretical background of the mathematical approaches will be presented in the following sections.

2 Physiological Background

The central aspect of the endocrine system and starting point of signaling pathways is located in the brain and consists of the hypothalamus and pituitary gland leading to the stimulation of target glands such as the thyroid gland. This sequence of stimuli will be referred to as the Hypothalamus-Pituitary-Thyroid-axis (HPT-axis) and is responsible for maintaining overall homeostasis of the human body. Additionally, vital functions including brain development, metabolism, and regulating the cardiac cycle are associated with the HPT-axis, which makes the presence of diseases all the more consequential. The production of thyroid hormones is initialized by the hypothalamus and its release of Thyrotropin-Releasing Hormone (TRH) in the hypophysiotropic neurons. Afterwards, TRH is transported through blood vessels in the infundibulum, the connection between the hypothalamus and pituitary gland. Thereby, the thyrotrophs located in the anterior pituitary are stimulated, which leads to the production of Thyroid-Stimulating Hormones (TSH). The thyroid gland is located above the collar and below the larynx, consisting primarily of follicular cells. TSH connects to the outside membrane of these cells and initializes the transcription of a protein called thyroglobulin, which after additional processes leads to the release of the thyroid hormones Triiodothyronine (T3) and Thyroxine (T4). Serum concentrations of the thyroid hormones are regulated by a negative feedback loop, which means that the production of TRH and subsequently TSH will cease if a certain threshold is reached in the blood stream. According to [9], thyroid hormones T3 and T4 are produced in the ratio 1:10 and occur in the blood as bound or unbound moieties. Through this connection to plasma proteins called Thyroxin Binding Globulin (TBG) the half-life of thyroid hormones is prolonged to approximately 1 day for T3 and 7 days for T4. About 1% is freely distributed in the blood, therefore unbound, making them biologically more active.

3 Mathematical Models of the Thyroid Gland

Since Danzinger and Elmergreen pioneered the use of non-linear differential equations to model the negative-feedback control of the HPT-axis in 1954 [10], numerous mathematical models have been developed to better understand the complex dynamics of this endocrine system. More recent publications include [11], [2], that account for diseases related to the thyroid gland e.g. hypothyroidism, Grave's disease or Hashimoto's thyroidism in the introduced mathematical models. Among these models, introduced models extend the base models by accounting a more general description of the HPT-axis.

3.1 Physiological Considerations

In the context of mathematically modeling the HPT-axis, free T4 (FT4) is of particular importance as this hormone is transformed through deiodinase to T3 in target cells such as liver or kidneys, which is responsible for the transcription of hormone-dependent genes. Unlike TSH, TRH is not considered in mathematical models as acquiring data for validation is hardly possible without invasive procedures. Thus, the Hypothalamus-Pituitary complex (HP-complex) is considered as single compartment and represented by the concentration of TSH in the mathematical models, see Fig. 1.

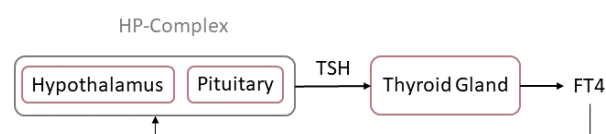


Fig. 1: Illustration of the aspects considered in modeling the HPT-axis.

Furthermore, the functionality of the thyroid gland is represented by the hormone concentration of FT4. There are different opinions in the scientific community about the normal range of hormone concentrations of TSH and FT4 in blood samples [12]. The considered normal ranges by the scientific community vary only slightly in the case of both hormones, therefore we choose the following as normal ranges given in Table 1.

Table 1: Normal ranges and units of TSH and FT4.

Hormone Concentration	Normal range	Unit
TSH	0.4 – 4	mU/L
FT4	7 – 18	pg/mL

Based on the model structure in Fig. 1, the following two models are considered and further analyzed through a sensitivity analysis.

3.2 Underlying Model

The first model we will consider, consists of four differential equations and describes the negative feedback loop of the HPT-axis in the case of the autoimmune disease Hashimoto's thyroiditis [13]. This disease is characterized by the presence of thyroid antibodies in blood samples, which attack and destroy the follicular cells of the thyroid gland and therefore cause hypothyroidism. According to [14], [15], Hashimoto's thyroiditis is the most common cause of hypothyroidism, affecting approximately 30% of patients with thyroid disorders. Patients with hypothyroidism can experience fluctuating body weight, fatigue, weakness and mood swings, which can significantly reduce their quality of life.

The model presented in [13] aims to incorporate significant characteristics of the disease Hashimoto's thyroiditis into the model the HPT-axis, which focus on the following assumptions stated in [13].

1. Anti-thyroid peroxidase antibodies recognize and attack the functional thyroid gland (precisely thyroid peroxidase (TPO) enzymes in the follicular cells).
2. The damaged part of the gland is no longer functional (active) in secreting thyroid hormones.
3. TSH stimulates the functional (active) part of the thyroid gland for growth and hormonal secretion.
4. TSH disappears from the blood through a non-specific excretion mechanism.
5. TSH distributes uniformly throughout the functional part of the gland.
6. The hypothalamus–pituitary function is intact.
7. The blood concentration of iodine is sufficient for synthesis of hormonal production.
8. The total TSH receptor concentration in the thyroid gland is unaffected in the presence of Hashimoto's thyroiditis. [16]

Based on this the system of differential equations is given by

$$\begin{aligned} \frac{dx}{dt} &= k_1 - \frac{k_1 y}{k_a + y} - k_2 x, & x(t_0) &= x_0, \\ \frac{dy}{dt} &= \frac{(k_3 z)x}{k_d + x} - k_4 y, & y(t_0) &= y_0, \\ \frac{dz}{dt} &= k_5 \left(\frac{x}{z} - N \right) - k_6 z w, & z(t_0) &= z_0, \\ \frac{dw}{dt} &= k_7 z w - k_8 w, & w(t_0) &= w_0, \end{aligned} \quad (1)$$

with initial conditions $x_0, y_0, z_0, w_0 \geq 0$ at time t_0 is introduced. The variables x, y, w represent the hormone concentrations of TSH, FT4 and Anti-Thyroid Peroxidase Antibodies (TPOAb) at time t in days respectively. Furthermore, z accounts for the functional (active) size of the thyroid gland since Hashimoto's thyroiditis reduces the size of the thyroid gland. The model also includes the parameters $k_i, N \in \mathbb{R}^+, i \in \{1, \dots, 8, a, d\}$. These parameters were derived from literature and simulation studies. A stability analysis of the system of differential equations (1) has already been carried out in [13]. Furthermore, through bifurcation a parameter is identified which indicates the transition from euthyroid states to disease states.

3.3 Reduced Model

The second mathematical model, derived from (1) and introduced in [8], aims to describe the HPT-axis in a healthy (euthyroid) state, without considering the effects of specific thyroid disorders. The original system of four differential equations (1) is reduced by omitting the equations in z and w resulting in the system of two differential equations given by

$$\frac{dx}{dt} = k_1 - \frac{k_1 y}{k_a + y} - k_2 x, \quad x(t_0) = x_0, \quad (2)$$

$$\frac{dy}{dt} = \frac{k_3 x}{k_d + x} - k_4 y, \quad y(t_0) = y_0, \quad (3)$$

with initial conditions $(x_0, y_0)^T$ with $x_0, y_0 \geq 0$. The variables x and y keep their original meaning, and the model parameters get reduced to $k_1, k_2, k_3, k_4, k_a, k_d \in \mathbb{R}^+$. Since the variable z is no longer considered, only the term $\frac{k_3 z}{k_d + x}$ in the second equation changes, whereas the rest remains unchanged. This is compensated by k_3 .

In [17], the reduced model has been the subject of much investigation as to whether it can be used to present clinical data through calibration of selected model parameters. Furthermore, the above model is similar to the differential equations introduced in [2], however, it does not include time-dependent model parameters. Similar to the analysis in [2], we perform a sensitivity analysis using the following mathematical theory.

4 Sensitivity Analysis

As mathematical models become increasingly complex, it becomes more challenging to understand how small errors or perturbations in the input data affect the simulation results produced by these models. The theory of sensitivity analysis deals with the changes in simulation results due to the variation of model parameters, which grants essential information regarding model development and design optimization [18]. Particularly in the context of calibrating model parameters to fit a mathematical model to real-world data, identifying model parameters that have a significant impact on model output is a critical step in the optimization process. Therefore, the theoretical background to conduct a local and global sensitivity analysis is introduced.

4.1 Local Sensitivity Analysis

The underlying approach of this subsection is based on [19] and introduces the theory of local sensitivity analysis, which refers to calculating derivatives of a solution to a differential equation with respect to

model parameters. The following representation of a system of differential equations is given by

$$\frac{\partial z(t, \theta)}{\partial t} = f(t, z(t, \theta), \theta), \quad (4)$$

with the function $z: I \times G \rightarrow \mathbb{R}^n$, $z = z(t, \theta)$ for $I \subseteq \mathbb{R}$, $G \subseteq \mathbb{R}^m$ open and $f: I \times \mathbb{R}^n \times G \rightarrow \mathbb{R}^n$ continuous and locally Lipschitz continuous with respect to z . The solution z and additionally the function f are dependent on the vector $\theta \in G$, which represents the model parameters. Furthermore, we assume that the solution z is partially differentiable in θ , which allows the approximation

$$z_k(t, \theta) - z_k(t, \theta^*) \approx \sum_{j=1}^m \frac{\partial z_k(t, \theta^*)}{\partial \theta_j} (\theta_j - \theta_j^*) \quad (5)$$

for a fixed parameter vector θ^* and $k = 1, \dots, n$ using Taylor's theorem. Thereby, the local sensitivity of the state vector z with respect to model parameters θ_j for $j \in \{1, \dots, m\}$ at time t is defined as

$$\frac{\partial z_k(t, \theta^*)}{\partial \theta_j}, \quad (6)$$

where θ^* is a given parameter. According to [19], a simple approach to calculate model sensitivities is the use of numerical differentiation given by

$$\frac{\partial z(t, \theta)}{\partial \theta_j} = \frac{z(t, \theta + \Delta\theta_j) - z(t, \theta)}{\Delta\theta_j} + \mathcal{O}(\Delta\theta_j) \quad (7)$$

for $j = 1, \dots, m$, where $\theta + \Delta\theta_j$ stands for the mathematical expression of only adding the value $\Delta\theta_j$ to the j -th component of θ . However, this method has some drawbacks as the accuracy of the approximation (7) strongly depends on the choice of $\Delta\theta_j$. As mentioned in [20], if $\Delta\theta_j$ is chosen unnecessarily large, the corresponding error term of the approximation becomes indecently large as well. If $\Delta\theta_j$ is set too small, the error can increase, as well due to floating point cancellations in the calculation.

To avoid these errors, Matlab toolbox for Sensitivity Analysis for ODEs and DAEs is used, as it employs a suitable strategy described in [20] for the calculation of $\Delta\theta_j$. The Matlab function `sens_sys` is used to compute the local sensitivities defined in (7). In the case the a local sensitivity analysis, only information about the influence of a single parameter is provided while the remaining parameters are fixed. To gain additional insight into the collective influence of parameters the global sensitivity analysis based on Sobol' indices is introduced in the following section.

4.2 Global Sensitivity Analysis

In contrast to local sensitivity, global sensitivity provides information about the collective influence of multiple model parameters. In that regard, the method of Sobol' is used, which conducts a global sensitivity analysis on the basis of variance decomposition, see [21], [22]. We consider a rudimentary modeling approach and assume, that each model can be described as

$$Y = f(\mathbf{X}) = f(X_1, \dots, X_n), \quad (8)$$

where $f: \mathbb{R}^n \rightarrow \mathbb{R}$, and Y represents the model output, which serves the simple propose of introducing the theory assumed to be a scalar, but higher dimensional output is permitted as well. Regarding the input $\mathbf{X} = (X_1, \dots, X_n) \in [0, 1]^n$, elements within the n -dimensional unit hypercube are considered, where the values (X_1, \dots, X_n) are uniformly distributed within $[0, 1]^n$. This condition may be assumed without loss of generality since any input space can be transformed to $[0, 1]^n$. Furthermore, we assume that the Hoeffding decomposition for the model output Y holds, and is given by

$$\begin{aligned} Y = & f_0 + \sum_{i=1}^n f_i(X_i) + \dots \\ & + \sum_{i=1}^n \sum_{j=i+1}^n f_{ij}(X_i, X_j) + \dots \\ & + f_{1, \dots, n}(X_1, \dots, X_n). \end{aligned} \quad (9)$$

A necessary condition for (9) to be fulfilled, is given by

$$\int_0^1 f_{i_1, i_2, \dots, i_s}(X_{i_1}, X_{i_2}, \dots, X_{i_s}) dX_{i_k} = 0, \quad (10)$$

for $1 \leq i_1 < i_2 < \dots < i_s \leq k$ and $i_k \in \{i_1, i_2, \dots, i_s\}$. This results in $f_0 = C$, where C is a constant. Additionally, (9) is unique and the summands are mutually orthogonal. The functions f_{i_1, i_2, \dots, i_s} are obtained by

$$\begin{aligned} f_0 &= \mathbb{E}(Y), \quad f_i = \mathbb{E}_{X_{\sim i}}(Y|X_i) - \mathbb{E}(Y), \\ f_{ij} &= \mathbb{E}_{X_{\sim ij}}(Y|X_i, X_j) - f_i - f_j - \mathbb{E}(Y), \end{aligned} \quad (11)$$

where higher-order terms follow the same pattern. The expression $X_{\sim i}$ refers to the set of all variables except X_i . Using the expressions defined in (11), the partial variances are denoted to

$$\begin{aligned} \mathbb{V}_i &= \mathbb{V}(f_i(X_i)) = \mathbb{V}_{X_i}(\mathbb{E}_{X_{\sim i}}(Y|X_i)), \\ \mathbb{V}_{ij} &= \mathbb{V}(f_{ij}(X_i, X_j)), \end{aligned} \quad (12)$$

in which case again higher order expression are obtained by following the same pattern. Based on (12) and assumption (9) an expression for the variance decomposition is achieved as

$$\mathbb{V}(Y) = \sum_{i=1}^n \mathbb{V}_i + \sum_{i=1}^{n-1} \sum_{j=i+1}^n \mathbb{V}_{ij} + \dots + \mathbb{V}_{1,\dots,n}.$$

Through the use of Sobol' sensitivity indices S_i, S_{ij} the variance contributions to the total variance of individual parameters and the variance accounting for the interaction between parameters are determined. The Sobol' indices are given by

$$S_i = \frac{\mathbb{V}_i}{\mathbb{V}(Y)}, \quad i = 1, \dots, n$$

$$S_{ij} = \frac{\mathbb{V}_{ij}}{\mathbb{V}(Y)}, \quad 1 \leq i < j \leq n \quad (13)$$

which denotes the ratio to of the corresponding partial variance to the total variance and are determined using a Python script. The calculation of Sobol' indices make it necessary to calculate a large variety of different numerical solutions for varying sets of parameters. Thereto, Python libraries such as SALiB and SciPy including functions like `saltelli.sample` and `solve_ivp`, are used.

5 Results

This section is based on [23] and presents the results of the local and global sensitivity analysis, starting with a graphical motivation. Understanding the effects of changes in the output of (2) and (3) due to variation in model parameters provides useful information about the extent to which the model is able to represent clinical data. First, a graphical motivation is given to investigate the parameter influence on a fundamental level.

5.1 Graphical Analysis

In this approach, the model parameters are changed individually and the corresponding solutions are plotted. The reduced model (2) and (3) is considered with initial conditions $(x_0, y_0)^T = (1, 13)^T$ for the starting concentrations of TSH and FT4 respectively. They are chosen in accordance with [13] and are situated within the normal ranges of the respective hormone. In the course of this graphical motivation the initial conditions of the differential equations (2) and (3) are not varied, only the underlying model parameters. The initial values of the model parameters $k_i \in \mathbb{R}^+, i \in \{1, 2, 3, 4, a, d\}$ are assigned to $k_1 = 5000, k_2 = 16.63, k_3 = 1.1262, k_4 = 0.099, k_a = 0.0434, k_d = 0.0021$ and taken from literature sources in [13] or in the case of the parameter k_3

results from [17] were taken into account. Since (2) and (3) originate from a larger system of differential equations, the omitted quantity of the thyroid size denoted as z in (3) is compensated by the value of k_3 . This consequence has been thoroughly discussed in [17] through the calibration of model parameters including k_3 to clinical data. To conduct a graphical presentation of the solutions of (2) and (3), the parameters are individually increased by a factor $s \in [0.1, 1000]$. For each set of model parameters, (2) and (3) are solved using the Matlab function `ode15s`. Each model parameter is increased twice, therefore resulting in three different solutions for each hormone concentration and each parameter. The resulting curves are displayed in Fig. 2 and Fig. 3.

The solution associated with the starting parameter set is represented by a continuous line, and those resulting from modified parameters by a dashed line. An increase of the model parameters k_1, k_4, k_a, k_d leads to an increase of the resulting solutions for TSH. The exact opposite can be observed for the model parameters k_2, k_3 . Even though the model parameters k_3, k_4, k_d are only contained in (3), their increase results in a noticeable change in the solutions of (2).

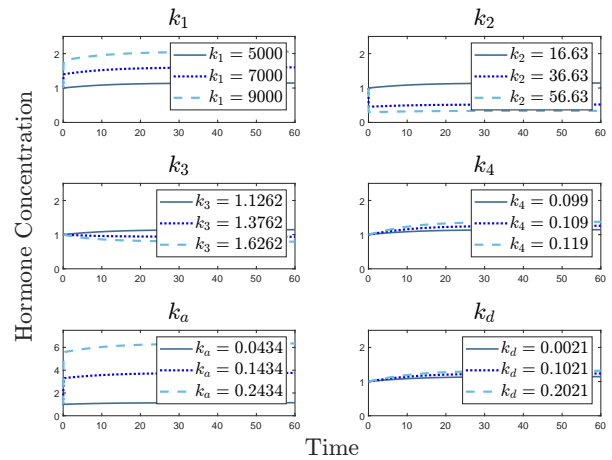


Fig. 2: Solutions of (2) with singularly varied model parameters $k_i, i \in \{1, 2, 3, 4, a, d\}$. The default values are $k_1 = 5000, k_2 = 16.63, k_3 = 1.1262, k_4 = 0.099, k_a = 0.0434, k_d = 0.0021$.

By comparison to the above observation, the model parameters k_1, k_2, k_a are only included in (2) and their alteration lead to no changes in the solutions of (3). This lies in contrast to the model parameters k_3, k_4, k_d , which influence the solution of both hormone concentrations, whereas the exact opposite can be observed for k_4 and k_a .

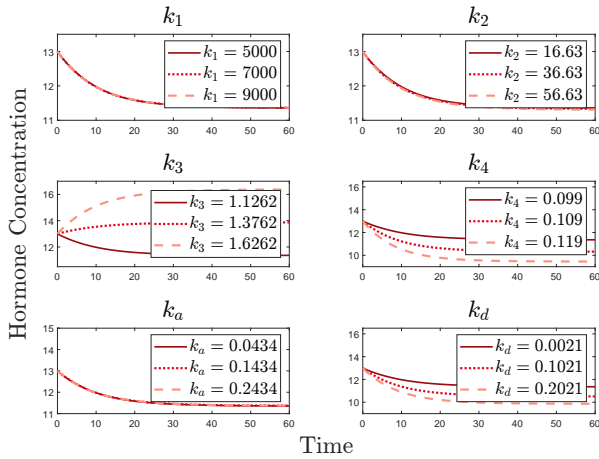


Fig. 3: Solutions of (3) with singularly varied model parameters k_i , $i \in \{1, 2, 3, 4, a, d\}$. The default values are $k_1 = 5000$, $k_2 = 16.63$, $k_3 = 1.1262$, $k_4 = 0.099$, $k_a = 0.0434$, $k_d = 0.0021$.

A first indication of the influence of model parameters on model output is provided by the graphical representation of different solutions with various underlying parameter sets.

5.2 Results of Local Sensitivity Analysis

To support the conclusions drawn from the previous section, a local sensitivity analysis is conducted. The Matlab function `sens_sys` included in the toolbox Sensitivity Analysis is utilized to calculate the local sensitivity introduced in (6) of the reduced model. The resulting local sensitivities $\frac{\partial x}{\partial k_j}$ and $\frac{\partial y}{\partial k_j}$ for $j \in \{1, 2, 3, 4, a, d\}$ are shown in Fig. 4 and the following influences on the solution are deduced.

Starting with the model parameters k_1 and k_a , the local sensitivities $\frac{\partial x}{\partial k_1}$, $\frac{\partial y}{\partial k_1}$, $\frac{\partial x}{\partial k_a}$ and $\frac{\partial y}{\partial k_a}$ show the same influence on the model output as indicated in the graphical motivation. We observe that the individual variation of the model parameters k_1 and k_a only lead to changes in the trajectories representing the hormone TSH whereas no change is observable in the trajectory representing FT4. Continuing with the model parameter k_2 , similar behavior to k_1 and k_a is noticeable. No change regarding the hormone concentration of FT4 is deduced from $\frac{\partial y}{\partial k_2}$ and an increase in the parameter value leads to a decrease of the trajectory representing TSH. In the case of k_4 and k_d , there is almost no influence on the resulting solution of TSH. However, the individual variation of these parameters leads to a decrease in the trajectory representing FT4. When k_4 is varied, the local sensitivity $\frac{\partial y}{\partial k_4}$ even indicates a significant change in the model output.

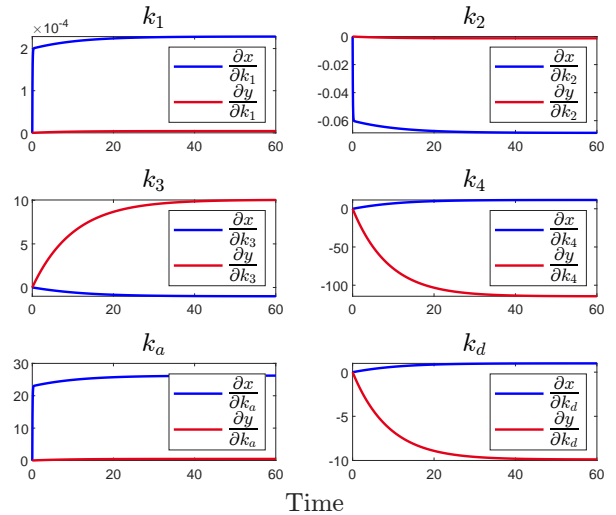


Fig. 4: Local sensitivities for all parameters $k_1, k_2, k_3, k_4, k_a, k_d$ included in (2) and (3). The sensitivities for the differential equations (2) and (3) representing the concentration of TSH and FT4 are represented in blue and red, respectively.

Lastly, similar to k_4 and k_a the variation of k_3 does not alter the trajectory representing TSH, however an increase of the parameter value leads to an increase in the solution of FT4.

5.3 Results of Global Sensitivity Analysis

The goal of conducting a global sensitivity analysis is to quantify the relative importance of each input variable on the value of an assigned output response [24]. First and second order Sobol' indices are calculated to quantify the contribution of each model parameter, or a combination of them, to the response variance decomposition [25].

The first step is to decide which parameters to include in the Sobol' analysis. The model parameters k_1, k_2 and k_4 are not included in the analysis as they are attributed to physiological properties such as secretion and excretion rate, therefore only the parameters k_3, k_a, k_d are included. Additionally, the contribution of the initial conditions $(x_0, y_0)^T$ is accounted for in the following global sensitivity analysis. In [17], the first measurement of a times series of clinical data were used as initial values for subsequent simulations of (2), (3), which varied widely. For this reason it is important to understand how the different initial values will affect the further course of the simulation. For the five selected parameters k_3, k_a, k_d, x_0, y_0 the following intervals for variation given in Table 2 are chosen due to the results of the graphical motivation and the respective normal ranges for the concentrations of TSH and FT4.

Table 2: Intervals considered for variation of the parameters k_3, k_a, k_d and initial conditions $(x_0, y_0)^T$ in the global sensitivity analysis.

Parameter	Variation Intervall
k_3	[1, 2]
k_a	[0.01, 2]
k_d	[0.001, 2]
x_0	[7, 18]
y_0	[2.5, 4]

Next, the Python function `saltelli.sample` is utilized to generate a certain amount of different sets of parameters k_3, k_a, k_d, x_0, y_0 . This amount is determined by $N \cdot (2D + 2)$, where N is a chosen value, in this case $N = 512$ and D stands for the number of parameters considered in the analysis, therefore $D = 5$. This results in a total of 6144 different sets of parameters. To generate a numerical solution of (2) and (3), the Python function `solve_ivp` is used to solve the mathematical model for each set of parameters generated by the function `saltelli.sample`. For the solution of the mathematical model a time interval of $t \in [0, 1000]$, unit in days, but only the last evaluation point is considered. The resulting first and second order Sobol' indices, determined using the function `sobolj.analyze`, are displayed in a heatmap, see Fig. 5.

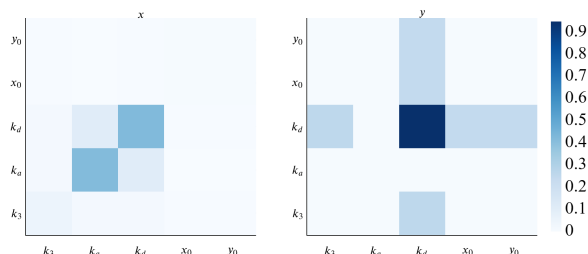


Fig. 5: Global sensitivities for model parameters k_3, k_a, k_d and initial values $(x_0, y_0)^T$ regarding (2) and (3). The Sobol' indices are displayed in a heatmap, the left graphic displays the results for TSH and the right for FT4.

The Sobol' indices for (2) and (3) are displayed in the left and right graphic of Fig. 5, respectively. We start with discussing the Sobol' indices for (2). Interestingly, the variation of the initial conditions $(x_0, y_0)^T$ in combination with any other considered parameter does not influence the output variance of the mathematical model in the case of TSH. In addition, the influence of the parameter k_3 is rather insignificant in comparison to k_a and k_d . The first order Sobol' indices, displayed generally on the diagonal, of k_a and k_d stand out in particular. To a

small extent, the combined variation of these two parameters lead to a variation of the output variance of (2).

The results of the global sensitivity analysis in the case of (3) representing the hormone concentration of FT4 displayed on the right hand side of Fig. 5 differ greatly from the results for TSH. In combination with the model parameter k_d , both initial conditions $(x_0, y_0)^T$ influence the response variance decomposition. Furthermore, the single variation of k_d results in a significant alteration of the output model variance, which is concluded from the first order Sobol' index. Even in combination with k_3 influential effects are observable.

Additionally, some further numerical examples regarding the global sensitivity analyses are presented in Fig. 6.

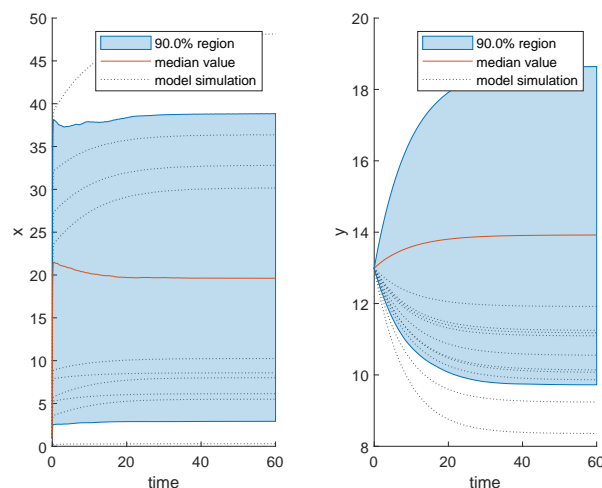


Fig. 6: Mean model response is displayed by the orange line, the shaded region on blue represents 90% of the simulation results and the dotted line additional simulation results.

Utilizing the Matlab function `sbiomodel`, the reduced mathematical model is implemented as SimBiology Model and afterwards the first- and total order Sobol indices are calculated using the function `sbiosobol`. These numerical results show that even a small variation of the parameters k_3, k_a, k_d in accordance with Table 2 lead to a significant variation of the model output.

6 Discussion

The primary objective of this scientific research comprises a local and global sensitivity analysis of a system of differential equations aiming to model the dynamics of the HPT-axis. The conducted analysis revealed key model parameters which strongly influ-

ence the model output. The hormone concentration of TSH is described through secretion minus excretion rate, where the secretion rate is described through two terms. The first term k_1 represents the maximum secretion rate of TSH and the second term $\frac{k_1 y}{k_a + y}$ accounts for the inhibition rate of FT4 present in the bloodstream using Michaelis-Menten kinetics [26]. The result that k_1 is a highly influential parameter is very plausible from a physiological point of view. Furthermore, variation of the model parameter k_a , which is also included in the term attributed to Michaelis-Menten kinetics, led to a change in the model output. Interestingly, the excretion rate k_2 has no effect on the model output in the case of TSH. Future research is necessary to relate the finding to physiological characteristics of the HPT-axis. According to the global sensitivity analysis and the resulting first order Sobol' indices, k_a and k_d equally influence the output variance of the mathematical model in the case of TSH, even though k_d is only included in the equation of FT4. This finding is to a certain extent in contradiction with the results of the local sensitivity analysis. The discrepancy may arise due to an insufficient sample number for the calculation of the Sobol' indices.

In the case of FT4, the hormone concentration is described using two terms, the secretion minus the excretion rate. In contrast to the excretion rate of TSH, the results of the local sensitivity analysis suggest that the excretion rate of FT4 k_4 is highly influential on the model output regarding FT4. In addition, the model parameters that are included in the Michaelis-Menten term also show an influence to a certain extent. This result aligns with the findings of the global sensitivity analysis, as the Sobol' indices suggest that the model parameter k_d has a strong influence on the output variation in the case of FT4. In addition, the second order Sobol' indices of k_d and all other considered parameters except k_a showed a significant influence. Further research is required to account for the influence of varying initial conditions on model output in the case of FT4 vs. TSH and the resulting physiological and clinical implications.

The findings concerning the model parameter k_1 align with previous studies [2], which partially also conducted a sensitivity analysis of a very similar system of differential equations describing the HPT-axis and incorporating thyroid diseases e.g. Hashimoto's thyroiditis, and Graves disease. However, in [2] only a partial sensitivity analysis is conducted for selected parameters, which are in addition time-dependent and dependent on the considered thyroid disease. The identification of significant

model parameters may lead to implications for understanding thyroid disorders. We concluded that small changes in certain parameters result in drastic changes in the output of the mathematical model. By understanding the characteristics of the model parameters, we aimed to put mathematical aspects into context with physiological and pathological conditions. However, in depth studies are necessary to gain further insight. Additionally, through clinical trials, this insight could suggest treatment strategies by managing thyroid-related diseases by targeting sensitive parameters. Despite the high potential and fundamental findings regarding the sensitivity analysis, further research is necessary to bridge the gap between model parameters and physiological and pathological characteristics. Additionally, the simplifications made in the model by assuming constant parameter values may overlook dynamic changes in the endocrine system.

In conclusion, the analysis of mathematical models of the HPT-axis is essential to understand its regulatory mechanisms and connect physiological characteristics with properties of the derived model. These findings enhance our understanding of thyroid regulation and pave the way for targeted therapeutic interventions. The outlook is to analyze models targeting different hormonal axes, such as the hypothalamus-pituitary-ovary axis, to combine different techniques in order to accurately depict clinical data.

Acknowledgment:

The authors would like to thank their research partner Prof. Dr. Michael Krebs from the Medical University of Vienna for his continued guidance in the field of endocrinology. Additionally, Lana Medo, Alexander Edthofer and Tünde Papp for proof reading and contributing their excellent advice.

References:

- [1] J.M. Kuyl, "The evolution of thyroid function tests", *Journal of Endocrinology, Metabolism and Diabetes of South Africa*, Vol.20, No.2, 2015, pp.11-16.
- [2] B. Yang, X. Tang, M. J. Haller, D. A. Schatz, and L. Rong, "A unified mathematical model of thyroid hormone regulation and implication for personalized treatment of thyroid disorders", *Journal of Theoretical Biology*, Vol.528, 2021.
- [3] M. Eisenberg, M. Samuels, and J. J. DiStefano III, "Extensions, Validation, and Clinical Applications of a Feedback Control System Simulator of the Hypothalamo-Pituitary-ThyroidAxis", *Thyroid* :

Official journal of the American Thyroid Association, Vol.18, 2008, pp.1071–1085.

- [4] J. Berberich, J. W. Dietrich, R. Hoermann, and M. A. Müller, "Mathematical modeling of the pituitary–thyroid feedback loop: role of a TSH-T3-shunt and sensitivity analysis", *Frontiers in endocrinology*, Vol.9, 2018, pp.1-11.
- [5] M. Pompa, et al., "A physiological mathematical model of the human thyroid", *Journal of Computational Science*, Vol.76, 2024.
- [6] M. K. Leow, "A mathematical model of pituitary–thyroid interaction to provide an insight into the nature of the thyrotropin–thyroid hormone relationship", *Journal of Theoretical Biology*, Vol.248, No.2, 2007, pp.275-287.
- [7] R. Sharma, V. Theiler-Schwetz, C. Trummer, S. Pliz., M. Reichhartinger, "Automatic Levothyroxine Dosing Algorithm for Patients Suffering from Hashimoto's Thyroiditis", *Bioengineering*, Vol.10, No.6, 2023.
- [8] S. Goede, "General review on mathematical HPT modeling General Review on Mathematical Modeling in the Hypothalamus Pituitary Thyroid System", submitted for publication.
- [9] M. Gekle, et al., *Taschenlehrbuch Physiologie*, Georg Thieme Verlag, 2015.
- [10] L. Danzinger, and G. L. George, "Mathematical theory of periodic relapsing catatonia", *Bulletin of Mathematical Biophysics*, Vol.16, 1954, pp.15-21.
- [11] M. C. Eisenberg, F. Santini, A. Marsili, A. Pinchera, and J. J. DiStefano, "TSH Regulation Dynamics in Central and Extreme Primary Hypothyroidism", *Thyroid*, Vol.20, No.11, 2010, pp.1215-1228.
- [12] J. S. Neves, et. al., "Thyroid hormones within the normal range and cardiac function in the general population: the epiporto study", *European Thyroid Journal*, Vol.10, No.2, 2021, pp.150-160.
- [13] B. Pandiyan, S. J. Merrill, and S. Benvenega, "A patient-specific model of the negative-feedback control of the hypothalamus-pituitary-thyroid (HPT) axis in autoimmune (Hashimoto's) thyroiditis", *Mathematical medicine and biology: a journal of the IMA*, Vol.31, No.3, 2014, pp.226-258.
- [14] F. Ragusa, et. al., "Hashimotos' thyroiditis: Epidemiology, pathogenesis, clinic and therapy", *Best Practice & Research Clinical Endocrinology & Metabolism* Vol.33, No.6, 2019.
- [15] L. Chiovato, F. Margi, A. Carlé, "Hypothyroidism in Context: Where We've Been and Where We're Going", *Advances in Therapy*, Vol.36, No.2, 2019, pp.47-58.
- [16] H. Tamaki, et. al., "Low prevalence of thyrotropin receptor antibody in primary hypothyroidism in Japan", *The Journal of Clinical Endocrinology and Metabolism* Vol.71, 1990, pp.1382-1386.
- [17] C. Horvath, A. Körner, and C. Modiz, "Data-based model identification of the hypothalamus-pituitary-thyroid complex", EUROSIM Congress 2023, to be published.
- [18] M. Koda, A. H Dogru, and J. H. Seinfeld, "Sensitivity analysis of partial differential equations with application to reaction and diffusion processes", *Journal of Computational Physics*, Vol.30, No.2, 1979, pp.259-282.
- [19] C. Rackauckas, et al., "A comparison of automatic differentiation and continuous sensitivity analysis for derivatives of differential equation solutions", in Proc. IEEE High Performance Extreme Computing Conference (HPEC), Waltham, 2021, pp.1-9.
- [20] R. L. Burden, J. D. Faires, and A. M. Burden, *Numerical Analysis*, Cengage Learning, 2015.
- [21] A. Saltelli, et el., "Variance based sensitivity analysis of model output design and estimator for the total sensitivity index", *Computer Physics Communications*, Vol.181, No.2, 2010, pp.259-270.
- [22] J. Nossent, P. Elsen, and W. Bauwems, "Sobol' sensitivity analysis of a complex environmental model", *Environmental Modelling and Software*, Vol. 26, No.12, 2011, pp.1515-1525.
- [23] C. Horvath, "Modelling and Analysis of the HPT-Complex", M.Sc. thesis, Intitute of Analysis and Scientific Computing, TU Wien, Vienna, 2023.
- [24] K. Cheng, Z. Lu, Y. Zhou, Y. Shi, and Y. Wei, "Global sensitivity analysis using support vector regression", *Applied Mathematical Modelling*, Vol.49, 2017, pp.587-598.

- [25] I. M. Sobol', "Global sensitivity indices for nonlinear mathematical models and their Monte Carlo estimates", *Mathematics and Computers in Simulation*, Vol.55, No.1, 2001, pp.271-280.
- [26] N. Chitnis, J. M. Hyman, and J. M. Cushing, "Determining important parameters in the spread of malaria through the sensitivity analysis of a mathematical model", *Bulletin of Mathematical Biology*, Vol.70, 2008, pp.1272-1296.

Contribution of Individual Authors to the Creation of a Scientific Article (Ghostwriting Policy)

Clara Horvath carried out the simulations and sensitivity analysis. She was also responsible for the literature review and research into the physiological context to establish a connection between mathematical models. Andreas Körner contributed with his expertise in modeling and simulation, supervised the process of writing this paper, and was responsible for proof reading.

Sources of Funding for Research Presented in a Scientific Article or Scientific Article Itself

No funding was received for conducting this study.

Conflicts of Interest

The authors have no conflicts of interest to declare that are relevant to the content of this article.

Creative Commons Attribution License 4.0 (Attribution 4.0 International , CC BY 4.0)

This article is published under the terms of the Creative Commons Attribution License 4.0

https://creativecommons.org/licenses/by/4.0/deed.en_US